CHAPTER IV
FACILE SYNTHESIS OF HIERARCHICAL N-RICH NANOPOROUS CARBON

4.1 Abstract

Nanoporous carbon has been prepared by pyrolysis of polybenzoxazine precursor in an inert atmosphere. The morphology of carbon particle was designed by varying the ratio of CTAB and silica template. The pyrolysis temperature was varied to obtain nitrogen-rich nanoporous carbon. The CO_2 activation at 800°C could improve the physical and chemical adsorption of this material. In addition, the elemental compositions on the surface of nanoporous carbon were analyzed by x-ray photoelectron spectroscopy. The autosorp AS1-MP was used to determine the surface area and particle size of the resulting nanoporous carbon. It was found that using 40% wt. of silica as a template, the nanoporous carbon exhibited the highest surface area. However, increasing % wt. of silica over this point would result in the agglomeration, confirmed by SEM micrographs. Moreover, the porous carbon contained both microporous and mesoporous structures. In this research, the effect of varying pyrolysis temperature to obtain nitrogen-rich nanoporous carbon which exhibited good CO_2 adsorption performance with high nitrogen content and high surface area was studied.

Keywords: Polybenzoxazine/ Nanoporous carbon/ CO_2 storage

4.2 Introduction

Nowadays, serious environmental problems owing to discharging of many pollutants from the combustion of various substances in forms of solids, liquid, and gas, have been reported as major global warming problems involving not only pollutants such as NO_x, SO_x and soot, but also greenhouse gases like carbon dioxide. The gas released from the combustion in the petrochemical industries is generally called flue gas. The composition of flue gas depends on what is being burned, but it will usually consist of mostly nitrogen and the next largest part of the flue gas is carbon dioxide (CO_2). Carbon dioxide is considered to be the primary greenhouse gas that is produced by combustion of coal or hydrocarbons leading to the warming of the earth's atmosphere and the environmental problem observed over the past 50 years [1]. During the last decade, the development of new technologies and materials for CO_2 capture and storage has been gaining increasing attention.

Nanoporous carbon is one of the selected materials that has many uses in various fields especially, CO_2 adsorption or storage because of its efficiency to adsorb and interact with atoms, ions and molecules on its large interior surfaces and in the nanometer sized pore space. Nanoporous materials as a subset of nanostructured materials have been a focus of nanoscience and nanotechnology that possess unique porosity, surface area, stable pore structural, high thermal stability and light weight [2]. Recently, studied the CO_2 capture from flue gas and discussed the effect of a nitrogen-functionalized porous material was obtained through pyrolysis of a porous polymer that prepared from terephthalaldehyde and melamine. This nitrogen-rich porous carbon exhibited more adsorption capacities [3].

Polybenzoxazine is a relatively novel class of addition-cure thermosetting phenolic resin that possess various advantageous characteristics such as excellent dimension stability, high thermal stability, low viscosity which can assist the film fabrication, no by-product released upon polymerization, high char yield and also rich molecular design flexilbility [4]. Moreover, polybenzoxazine has unique properties which are low water absorption despite having many hydrophilic groups and near zero shrinkage after processing [5]. Polybenzoxazine precursors have been synthesized from various aromatic / aliphatic amines, mono / diphenols, and formaldehyde [6]. In present work, we studied the pyrolysis polybenzoxazine

precursor which synthesized by Bisphenol-A, Formaldehyde and Tetraethylenepentamine (TEPA) via sol-gel process in an inert atmosphere [7]. In order to increase the pore volume by hard template synthesis method, the concentration of silica and Hexadecyltrimethylammonium bromide (CTAB) used as a surfactant were varied to obtain nanoporous carbon with high surface area containing both micro and mesoporous structure. Moreover, the effect of varying pyrolysis temperatures to obtained nitrogen-rich nanoporous carbon was also investigated.

4.3 Experimental

4.3.1 Materials

All chemicals were used without further purification. Bisphenol-A (97% purity) purchased from Sigma-Aldrich, formaldehyde (37 wt.% in water) purchased form Merck, tetraethylenepentamine (>80% purity) purchased from Fluka were used as starting materials for polybenzoxazine synthesis using N,N-Dimethylformamide (DMF) was purchased from Labscan Asia Co., Ltd., Thailand as a solvent. Cationic stabilizer, Hexadecyltrimethylammonium bromide [$CH_3(CH_2)_{15}N(Br)(CH_3)_3$, CTAB, $\geq$96.0%], was purchased from Fluka. LUDOX AS-40 colloidal silica solution (40%) with particle size of 24 nm was purchased from Aldrich. Ethanol (Absolute) was purchased from Labscan Asia Co., Ltd., Thailand. Hydrofluoric acid (HF, 48%) was purchased from Merck Limited, Germany.

4.3.2 Measurements

The thermal behavior of the polybenzoxazine precursor and fully-cured polybenzoxazine were analyzed by using a Perkin-Elmer DSC 7 instrument. The sample was heated from 30 to 300 °C with heating rate 10 °C/min under nitrogen gas with flow rate 20 ml/min. Thermogravimetric analysis was analyzed by using Perkin Elmer Thermogravimetric/Differential Thermal Analyzer (TG-DTA). The sample was heated from 30 to 800 °C under nitrogen gas with flow rate 50 ml/min. and heating rate 10 °C/min. The pyrolyzed temperature of polybenzoxazine was investigated from the onset temperature whereas char yield as the weight residue at 800 °C was reported. Moreover, nanoporous carbon without silica template could ensure by heating from 30 to 800°C under oxygen gas with flow rate 50 ml/min. and heating rate 10 °C/min. The functional groups related to structure of materials were investigated by using FT-IR technique. The FT-IR spectra of benzoxazine precursor and fully-cured polybenzoxazine were obtained using a Nicolet Nexus 670 FT-IR spectrometer in the frequency range of 4000-400 cm-1 with 64 scans at a resolution of 2 cm-1. KBr pellet technique was applied in the preparation of powder samples. Microstructure and surface morphology of nanoporous carbon materials were observed by a field emission scanning electron microscope (FE-SEM; HITACHI S4800) at voltage of 15 kV. The specimens were coated with platinum under vacuum

before observation to make them electrically conductive. Furthermore, the amount of silica template on the surface can be determined by Energy Dispersive X-Ray Spectrometer (EDX) mode. BET surface area, total pore volume, and average pore diameter of polybenzoxazine-based nanoporous carbon were determined by the N_2 physisorption using a Quantachrome Autosorb-1 MP surface area analyzer on the Brunauer-Emmett-Teller (BET) and Barret-Joyner-Halenda (BJH) methods, respectively. The X-ray diffractrometer (XRD) patterns of the nanoporous carbon were carried out on a Rigaku DMAX 2200HV using CuKα radiation(λ=0.154 nm) at 40 kV and 30 mA, scan speed of 5 /sec, and 2□ of 10 to 80. X-ray photoelectron spectroscopy, XPS (Kratos Axis Ultra DLD) was used to determine the oxidation states of N1s. A monochromatic AlKa was used as an X-ray source (anode HT = 15 kV). The residual pressure in the ion-pumped analysis chamber was lower than 5 x107 torr. The binding energies were referenced to the C1s peak (284.6 eV) to account for the effects of charging.

4.3.3 Methodology

4.3.3.1 Synthesis of Benzoxazine precursor

Benzoxazine precursors were synthesized by dissolving Bisphenol-A in N,N,-dimethylformamide (DMF) in the glass bottle and stirred continuously until the clear solution was obtained. Formaldehyde solution was then added into the bisphenol-A solution and mixed with various silica colloids and CTAB (cetyltrimethylammonium bromide) respectively. After that Tetraethylenepentamine (TEPA) in DMF was added dropwise into the mixture solution and stirred continuously for approximately 1 hour before putting in a closed system and heating at 80°C for 2 days in an oil bath to let the gel set. After that, CTAB and solvent were removed by ambient pressure drying (Soxhlet Extraction). The synthetic reaction is shown in Figure 5.1 by the molar ratio of bisphenol-A : formaldehyde : TEPA was 1:4:1.

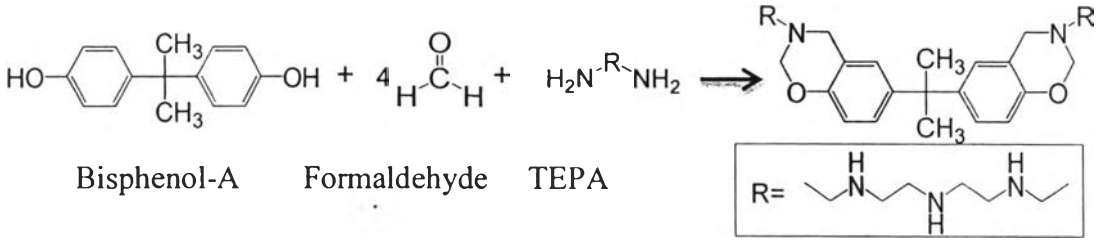

Scheme 4.1 Preparation of polybenzoxazine precursor.

4.3.3.2 Curing of Benzoxazine Xerogel

The obtained organic xerogel was then fully cured by step curing in an oven at room temperature to 100 °C in 30 min, 100 to 200 °C in 8 hr, holding at 200 °C for 3 hr, 200 to 220 °C in 30 min, holding at 220 °C for 15 min, and finally cooling down to room temperature.

4.3.3.3 Pyrolysis Process

Polybenzoxazines were pyrolyzed under nitrogen flow rate of 500 cm^3/min. The pyrolysis temperatures varied in four conditions were 400, 500, 600 and 800 °C. The heating profile was as follows: heating from room temperature to 200 °C in 1 hr, 200 to varies pyrolysis temperatures and holding each pyrolysis temperatures for 2 hr and finally cooling down to room temperature.

4.3.3.4 Silica Removal

Silica colloids were removed from carbon xerogels (CX) by immersing in 15% wt hydrofluoric acid for 24 h.

Preparation of 15% wt of HF

Mixed solvents = EtOH:H_2O = 50:50 (mass ratio)

Total weight of mixed solvent = 200 g (From EtOH 100 g and H_2O 100 g)

Calculation

$$\frac{\text{HF}}{\text{200 g of mixed solvents + HF}} \times 100 = 15\% \text{ wt of HF solution}$$

$$\text{HF} = 35.29 \text{ g}$$

However, the commercial HF solution bought is 48% wt in water. Therefore, 35.29 g HF can be calculated from the following equation:

$$\frac{35.29 \times 100}{48} = 73.52 \text{ g}$$

In addition, the amount of water in 73.52 g of 48% wt HF solution is 73.52-35.29 = 38.23 g.

Therefore, the amount of water added is 100.00-38.23 = 61.77 g

The preparation of 15 % wt of HF aqueous solution can be prepared as the following formula

100 g EtOH : 61.77 g Water : 73.52 g of 48% wt HF solution

After that, the solution of 15% HF will be weighted for etching PBZ-Silica composite. The amount of 15% wt HF solution used, comparing to amount of PBZ-Silica, can be calculated by the following mass ratio:

$$\frac{\text{Weight of mixed solvent}}{\text{Weight of PBZ-Silica}} = 100$$

The 48% of HF solution shows the density of 1.16 g/cc.
73.52 g of 48% wt HF solution can be calculated in term of volume

$$\frac{73.52 \text{ g}}{1.16 \text{ g/cc}} = 63.38 \text{ cc} \quad (V = m/D)$$

4.3.3.5 CO_2 Adsorption process

A pressure transmitter was installed to measure pressure of the system. One gram of the prepared adsorbent was loaded into the stainless steel adsorption chamber, which was heated by the furnace in order to reach the adsorption temperatures. He (Ultra high purity, Praxair Inc.) was used as a purge gas in this study. The adsorption processes were carried out using high purity CO_2 gas (99.99%) at pressure 20 psi. The temperature of the adsorption chamber was adjusted and maintained by an internal temperature sensor.

4.4 Results and Discussions

4.4.1 Characterizations of Benzoxazine Precursors and Polybenzoxazines

The chemical structure of benzoxazine precursors and polybenzoxazine were investigated by FTIR technique. The FTIR spectra of benzoxazine precursors were shown in Fig 1 (a). The characteristic absorption band of partially-cured benzoxazine was observed at 1490-1500 cm^{-1} for tri-substituted benzene ring. The band at 1260-1265 cm^{-1} represents asymmetric stretching of C-O-C of oxazine. The asymmetric stretching of C-N-C was observed around 1180-1187 cm-1. The out of plane bending vibration of C-H was observed around 920-950 cm-1. In case of fully cured polybenzoxazine that polymerized at 220 °C, the intensity of those absorption bands disappeared because the ring-opening of benzoxazine was completed as shown in Figure (b). These results are corresponding with the study of Katanyoota [8] and Takeichi [9], suggesting that the peak disappearance is due to the ring-opening polymerization of the benzoxazine precursor.

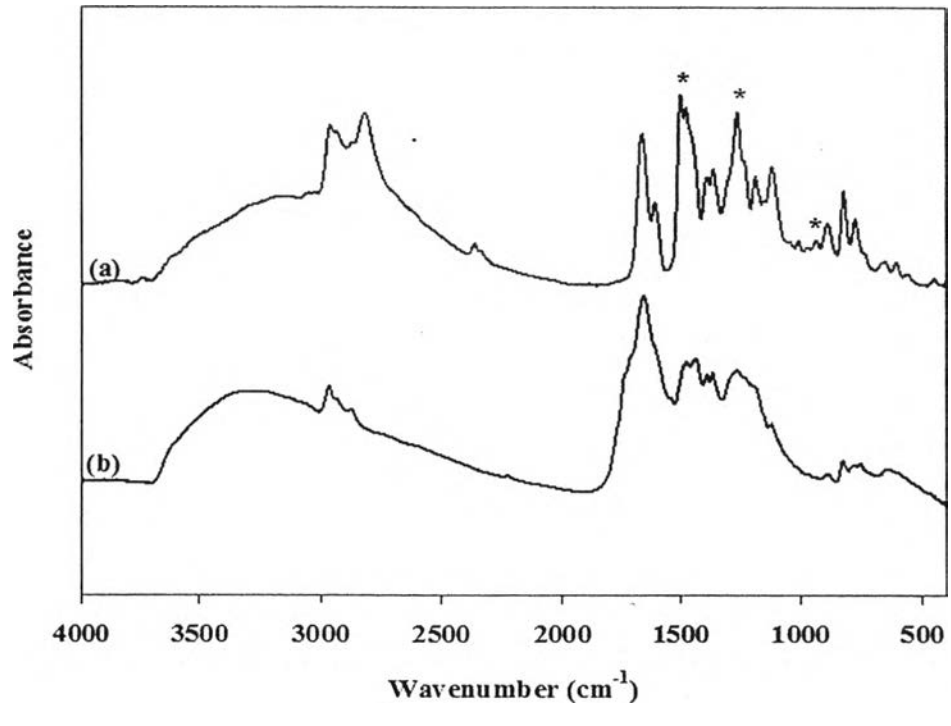

Figure 4.1 FTIR spectra of TEPA-based benzoxazine precursor (a) and the poly-Benzoxazine (b).

4.4.2 Thermal Properties of Benzoxazine Precursors and Polybenzoxazines

4.4.2.1 Thermal Properties of Benzoxazine Precursors

The curing step of benzoxazine precursor has been investigated by differential scanning calorimeter (DSC7, Perkin Elmer). The DSC thermogram shows the exothermal peaks of benzoxazine precursor started from 170 to 270°C with a maximum at 256°C, corresponding to the benzoxazine ring opening polymerization as seen from the Fig 4.2 (a). While the exothermic peak after heat treatment at 220 °C, the fully cured polybenzoxazines were obtained corresponding with the completely disappeared exothermal peaks of polybenzoxazine because oxazine ring-opening process was completed as shown in Fig 4.2 (b). This result was similar to that reported by Takeichi and coworker [9]. Moreover, it is corresponding with decreasing intensity of tri-substituted benzene ring and out of plane bending vibrations of C-H in IR spectra as shown in Fig 4.1.

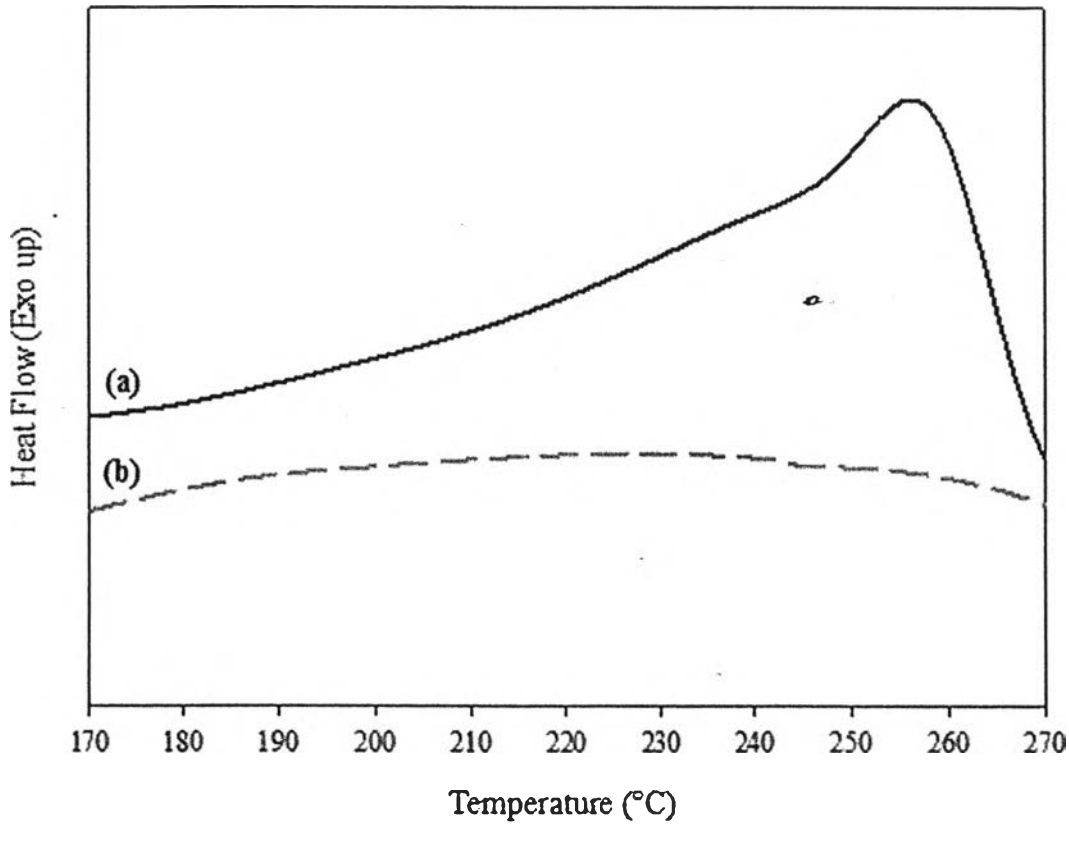

Figure 4.2 DSC thermograms of the benzoxazine precursor after drying at 80 °C (pre-cured) (a) and after heat treatment at 220 °C (fully-cured) (b).

4.4.2.2 Thermal Properties of Polybenzoxazines

Thermal stability of benzoxazine precursor and polybenzoxazine with colloidal silica as hard a template was examined by thermal gravimetric analysis (TGA) under nitrogen atmosphere. The silica nanoparticle content of PBZ composites was varied in the range of 10-50 wt%. The decomposition temperatures were further used to evaluate the appropriate temperature for pyrolysis into porous carbon. The fully-cured polybenzoxazine started to decompose at approximately 280 °C and the char yields at 800 °C was around 35 % as shown in Fig 3 As reported by Hemvichian and co-worker, in which the decomposition of polybenzoxazine was investigated by the TGA-GC-MS technique, proving that the decomposition occurred due to the degradation of polybenzoxazine[10]. In case of PBZ-silica composite xerogels, when silica particles were added, the thermal stability was increased as well as the char yields. implying that silica nanoparticles were successful incorporated into PBZ xerogels and the thermal stability was improved when increasing amount of silica nanoparticles [11].

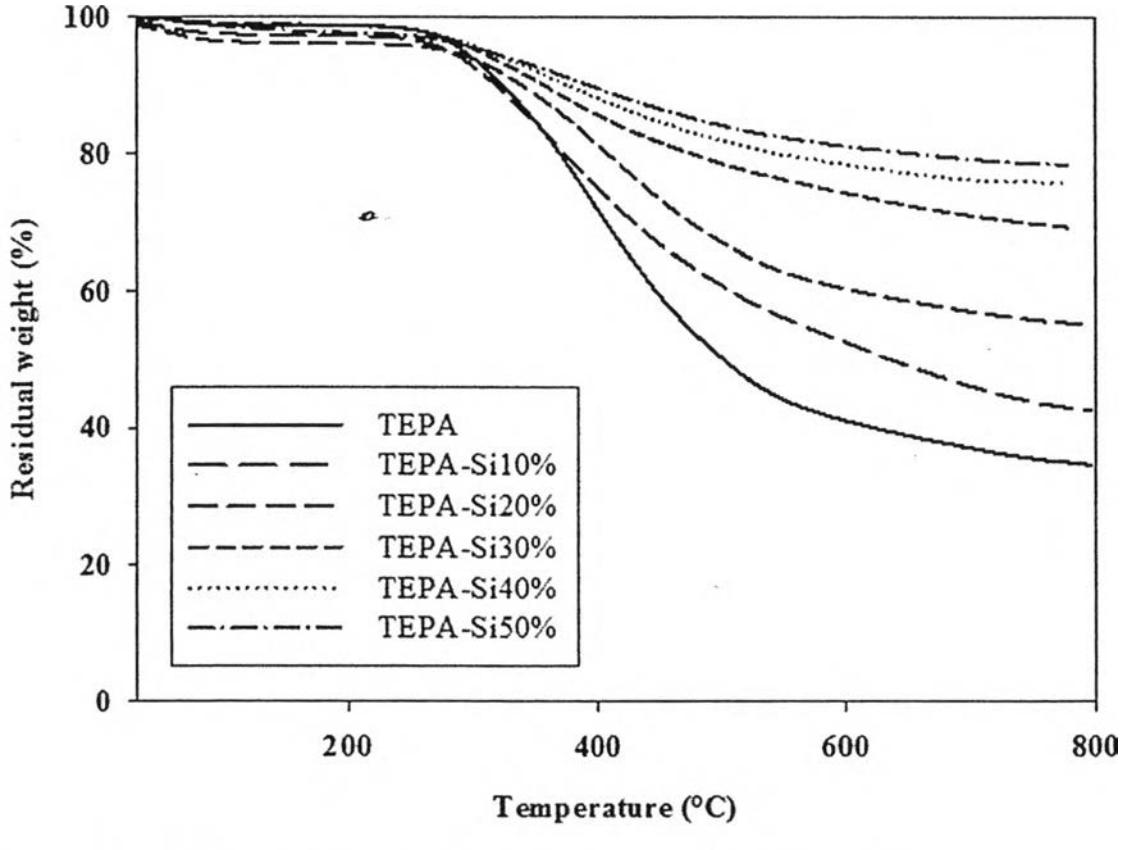

Figure 4.3 TGA thermograms of polybenzoxazines with silica template.

Table 4.1 The char yields (wt%) of polybenzoxazines

Polyenzoxazine	Char yield (wt%)
PBZ	35
PBZ+Si 10%	42
PBZ+Si 20%	55
PBZ+Si 30%	69
PBZ+Si 40%	76
PBZ+Si 50%	78

4.4.2.3 Etching process of nanoporous carbon

In order to confirm etching process for removing silica contents out of nanoporous carbon, carbon xerogel after etching process was investigated by TG-DTA in oxygen atmosphere. The result of thermogram shown that the char yield of nanoporous carbon is approached to 0 wt%, indicating that all silica contents were removed after etching process.

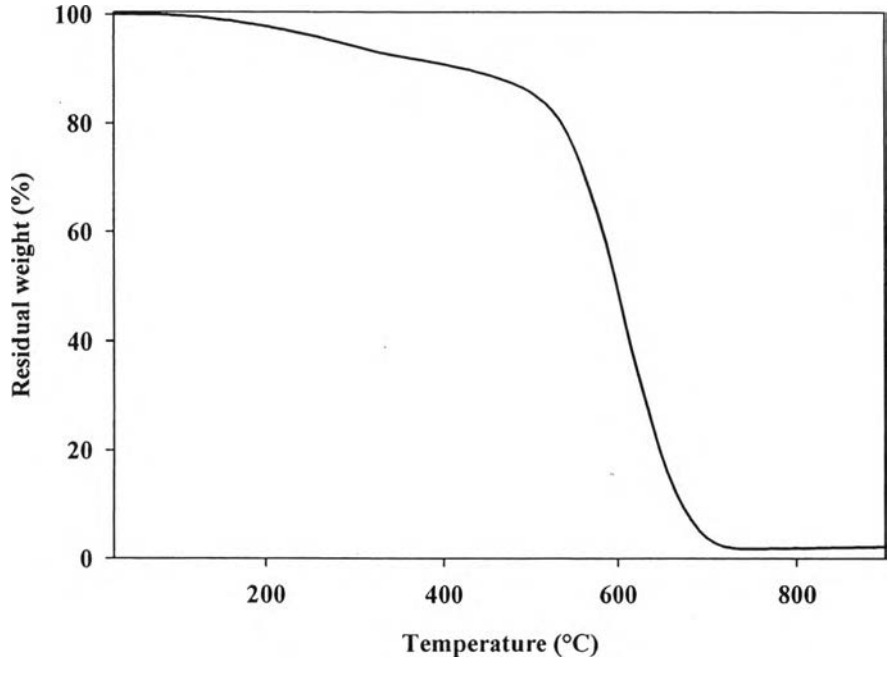

Figure 4.4 TGA thermograms of carbon xerogel after etching process.

4.4.3 Morphology of Nanoporous Carbon by SEM

4.4.3.1 Morphology of Silica-Impregnated Carbon

The morphology of nanoporous carbon and nanoporous carbon incorporated with silica was observed by Scanning electron Microscope (SEM). The SEM micrographs reveal the pore structure of nanoporous carbon prepared from polybenzoxazine with different Si loading (10, 20, 30, 40, and 50 % by weight). The pore structure of nanoporous carbon composed of interconnected particles in three-dimension network containing continuous micropores and mesopores. The image of nanocarbon xerogel without silica template exhibits a structure like a circular shape. As increasing the concentration of silica, carbon xerogels were slightly hard to distinguish in shape and form because silica as a template would embed in carbon xerogels. When increasing up to 40%wt of silica, the SEM micrograph showed silica nanoparticle circular shape was well distributed in nanoporous carbon due to the stabilization of cationic surfactant (CTAB) as shown in Fig 4 However, at 50%wt of silica, the silica particles were agglomerated and inverse phase took place because the direct mutual attraction between particles via Van Der Waals forces or hydrogen bonding. As expected, the aggregation was increased with the increasing of Silica nanoparticles. So, we can conclude that the composite yield from TG-DTA technique and SEM micrographs can confirm the successful incorporation of silica nanoparticles into nanoporous carbon structure.

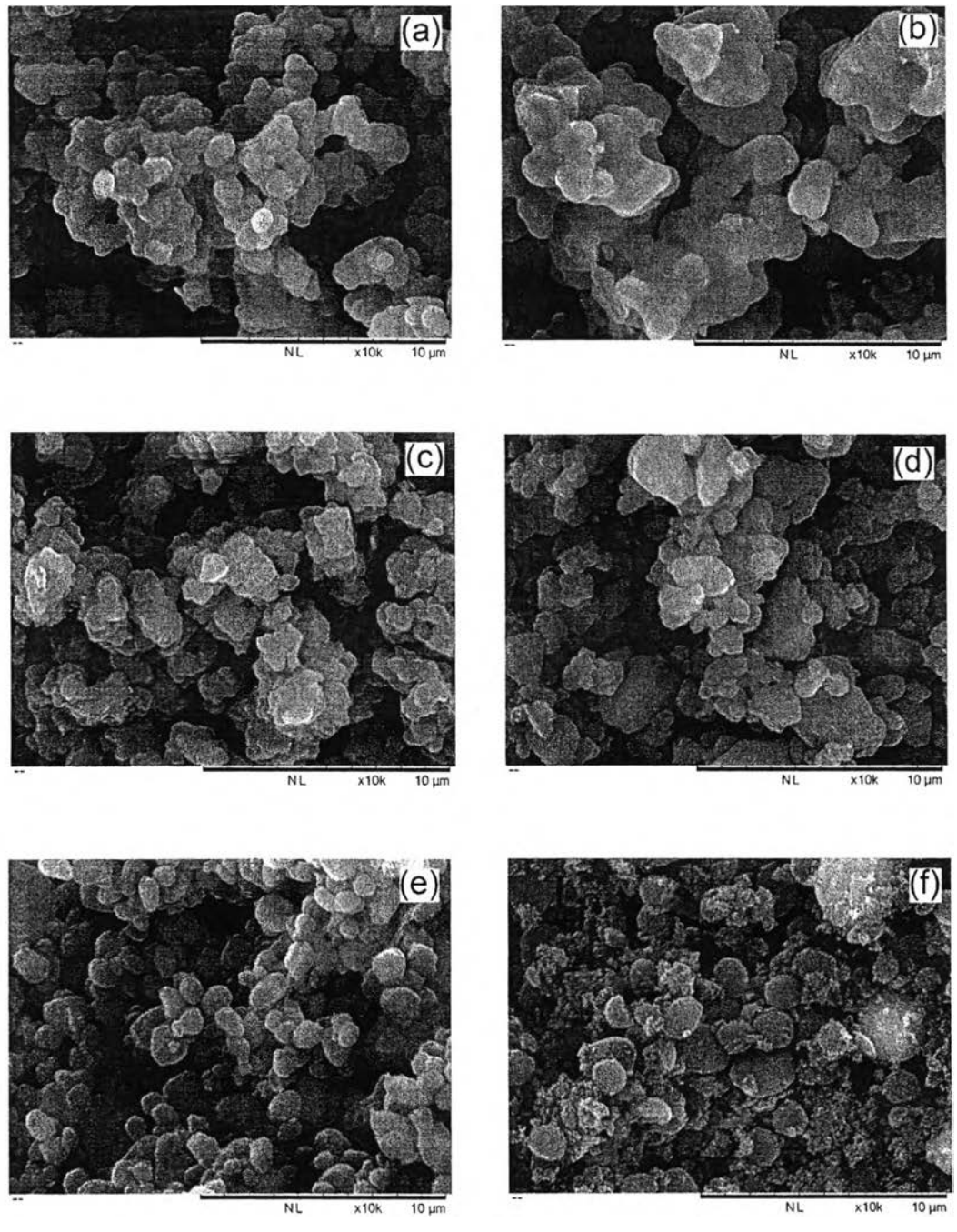

Figure 4.5 Morphology of nanoporous carbon - based polybenzoxazine: nanoporous carbon without silica template (a), nanoporous carbon with silica template loading 10% (b), 20% (c), 30% (d), 40% (e), and 50% (f).

4.4.3.2 Morphology of Activated Nanoporous Carbon

To compare between morphology of activated nanoporous carbon without silica templating and activated nanoporous carbon with silica templating, SEM was used. After activation under CO_2 atmosphere, microstructure was generated on the surface as shown in Fig.5(c). Moreover, the SEM micrograph exhibits that activated nanoporous carbon with silica has rougher surface than activated nanoporous carbon because of the removal of the silica template which generated pore on the surface as shown Fig.5 corresponding with the resulting BET surface area.

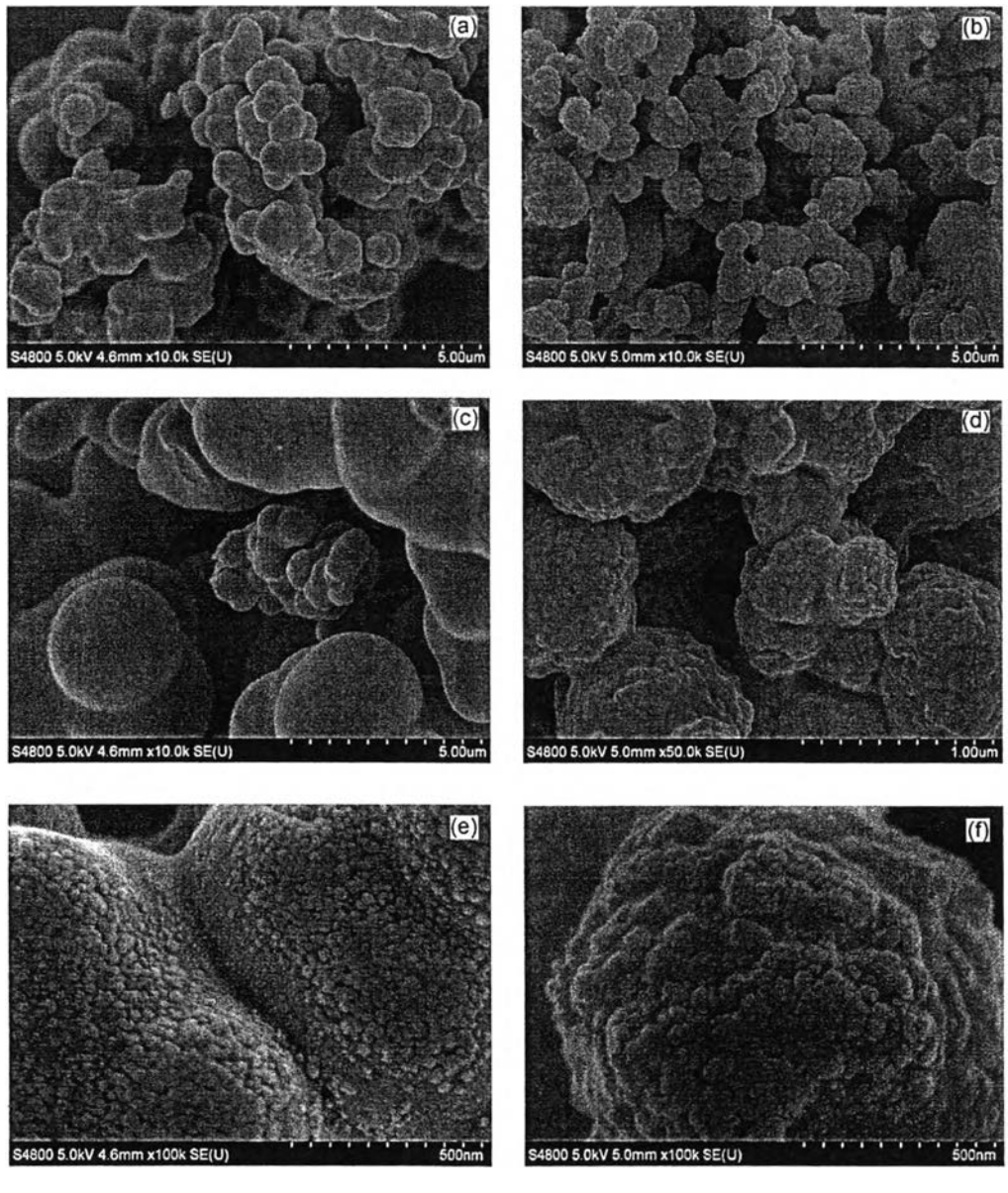

Figure 4.6 Morphology of activated nanoporous carbon without silica template (10k) (a), activated nanoporous carbon with silica template (10k) (b), activated nanoporous carbon without silica template (50k) (c), activated nanoporous carbon with silica template (50k) (d), activated nanoporous carbon without silica template (100k) (e), and activated nanoporous carbon with silica template (100k) (f).

4.4.4 Surface Area Characteristics of Nanoporous Carbon

The specific surface area, total pore volume, and average pore diameter of polybenzoxazine-based nanoporous carbon using silica as a hard template were determined by the N_2 physisorption using a Quantachrome Autosorb-1 MP surface area analyzer. Before analysis, the samples were heated in vacuum atmosphere at 250°C overnight to eliminate volatile species that had adsorbed on the surface. The surface and pore characteristics of nanoporous carbon pyrolyzed at 600°C has lower surface area than nanoporous carbon pyrolyzed at 800°C. The results are summarized in Table 4.2-4.3. It was found that the average pore size in all sample are between 2-50 nm classified as a mesoporous material. Nanoporous carbon from polybenzoxazine without silica has BET surface area of 124 m^2/g and average pore size 7.17 nm. By using the colloidal silica particles with diameter of 24 nm some resulting porous carbon were found to have the pore size equals to that of the silica templates. The nanoporous carbon from polybenzoxazine with 40%wt of silica shows the highest BET surface area of 945 m^2/g and average pore size 15.44 nm. The nanoporous carbon from polybenzoxazine with 50%wt of silica has lower surface area than that of 40wt% of silica because high content of silica particle would cause agglomeration. After removal of silica, nanoporous carbon has large pore size; as a result the BET surface area would decrease. These results imply that silica can be used to improve the specific surface area and total pore volume by adding in a proper concentration.

Table 4.2 Surface area, total pore volume, and average pore diameter of nanoporous carbon pyrolyzed at 600°C derived from polybenzoxazine by using silica as a hard template

Sample name	Surface area (m^2/g)	Total pore volume (cm^3/g)	Average pore size (nm)
PBZ (blank)	124	0.031	7.17
PBZ+Si 10%	250	0.36	13.69
PBZ+Si 20%	522	0.78	15.47
PBZ+Si 30%	649	1.24	31.26
PBZ+Si 40%	687	2.28	29.48
PBZ+Si 50%	459	1.58	15.55

Table 4.3 Surface area, total pore volume, and average pore diameter of nanoporous carbon pyrolyzed at 800°C derived from polybenzoxazine by using silica as a hard template

Sample name	Surface area (m^2/g)	Total pore volume (cm^3/g)	Average pore size (nm)
PBZ (blank)	171	0.13	5.52
PBZ+Si 10%	255	0.32	13.67
PBZ+Si 20%	530	0.64	15.50
PBZ+Si 30%	808	1.21	15.40
PBZ+Si 40%	945	2.13	15.44
PBZ+Si 50%	741	3.81	29.39

4.4.5 The Order Structure of Nitrogen-Rich Nanoporous Carbons

The order structure of nitrogen-rich nanoporous carbons was investigated with the X-ray diffractrometer (XRD) measurement. To consider the crystalline structure of partially ordered carbon, the XRD technique was used to carry out the reflection peaks as shown in Fig.4.6a exhibiting the XRD pattern of nitrogen-rich nanoporous carbon pyrolyzed at 600°C. The diffraction peaks are observed broad peaks at $2\theta = 24°$ and 43°. From the d-spacing calculated by using Bragg's equation, these peaks can be index as the (002) and (100) reflection associated with graphitic carbon material [12-16]. When the carbonization temperature was increased to 800 °C, the diffraction peaks become narrow and shift to higher angles as shown in Fig.4.6b, revealing the order structure in graphitization form. This confirms that pyrolysis at 600 °C was enough to convert all organic contents into carbon form. The XRD results present that the nitrogen-rich nanoporous carbons were successfully obtained at various pyrolysis temperatures.

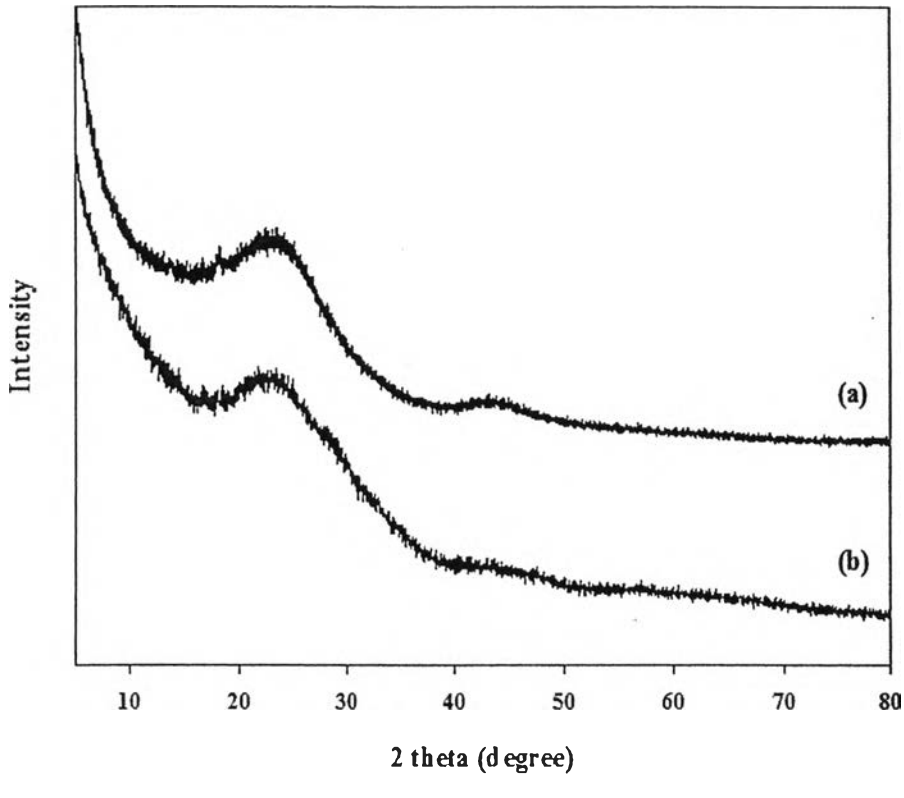

Figure 4.7 XRD patterns of nitrogen enriched carbons which carbonized at 600°C (a) and 800°C (b).

4.4.6 The Composition of Activated Nitrogen-Rich Nanoporous Carbons

In order to improve the adsorption capacity, the nitrogen species of N-containing adsorbent is considered to be an important role. The nature of the nitrogen species on the surface of the porous carbons was further investigated by XPS. The binding states of the N 1s photoelectrons of surface groups on nitrogen-rich nanoporous carbons were analyzed. The peak assignments for high resolution XPS of the prepared carbons are summarized in Table 3. Four intense peaks at 397.8, 398.9, 400.1 and 403.4 eV for nanocarbon with silica template loading 30% pyrolyzed at 600 °C (NC-30%-600 °C) can be distinguished, corresponding to secondary amine, NH_2-imine pyridine, pyrrole pyridone and N-oxide of pyridine-N, respectively [17-19]. N-oxide group (N-X) is determined on the surface, corresponding to the peak at 402.5–403.5 eV which probably generated by the oxidation of the sample due to the exposure to the ambient after activation process. In this work, the nitrogen enriched carbons pyrolyzed at 600°C exhibit peaks corresponding to pyridine and pyrrole type forms. Both pyrrole- and pyridine-type nitrogen have Lewis basicity, which can act as active sites for CO_2 capture [18, 19]. However, considering the high temperature of carbonization process, the peak of NH_2-imine pyridine disappeared because the high temperature may convert from pyridine-type to pyrrole-type structure [20].

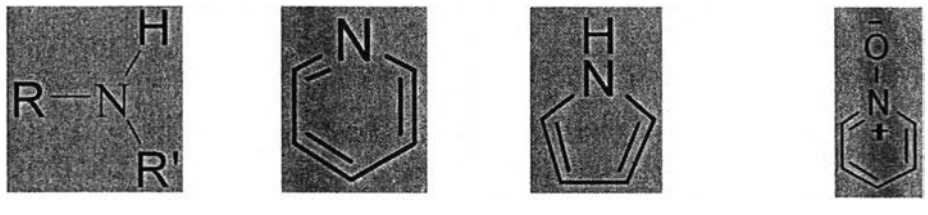

(a) Secondary amine (b) Pyridine (c) Pyrrole (d) Pyridine-N-oxide

Figure 4.8 The nature of nitrogen species on the surface of porous carbon; Secondary amine (a), Pyridine (b), Pyrrole (c), and Pyridine-N-oxide (d).

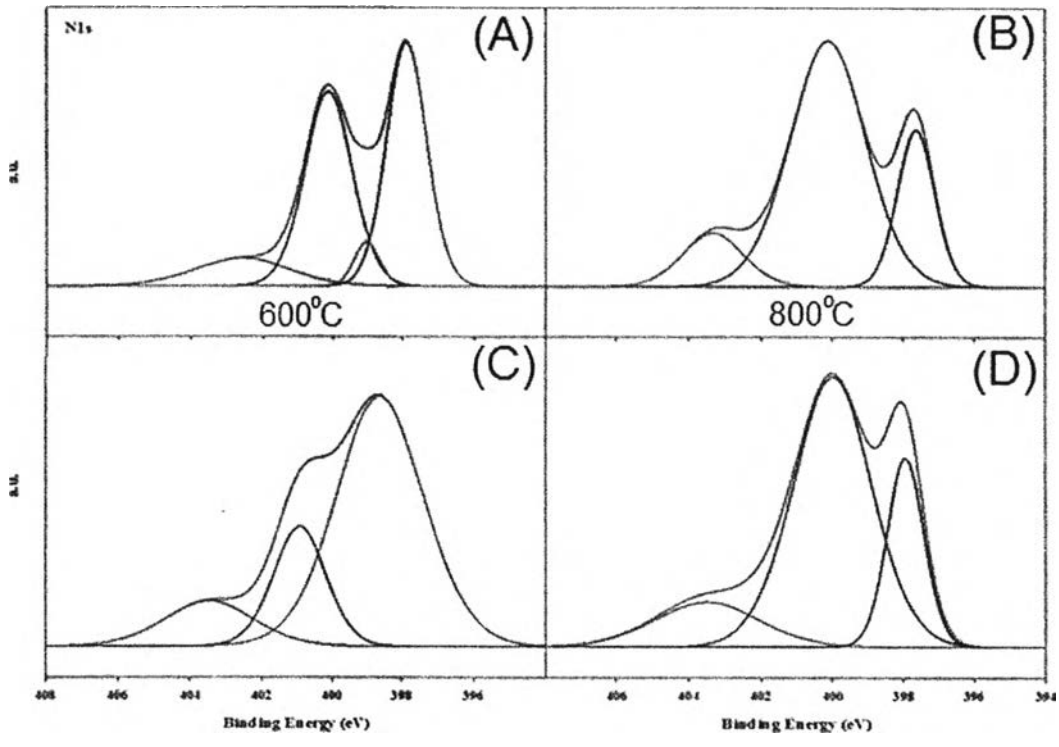

Figure 4.9 XRS pattern of NC-30-600 (nitrogen-rich nanoporous carbon with silica template loading 30% carbonized at 600°C) (a), NC-30-800, (b) NC-40-600 (c) and NC-30-800 (d).

Table 4.4 Distribution of N species obtained from the deconvolution of the N1s peak of different samples

Sample	Secondary amine	NH_2-imine pyridine	Pyrrole pyridone	N-oxide of pyridine-N
NC-30-600	397.8	398.9	400.1	403.4
NC-30-800	397.7	–	400.1	402.8
NC-40-600	–	398.5	400.1	403.5
NC-40-800	397.8	–	400.8	403.5

4.4.7 The Carbon-Dioxine Adsorption of Nitrogen-Rich Nanoporous Carbon

In order to measure the carbon-dioxide adsorption capacity, the activated nanoporous carbon has both microporous and mesoporous interconnected in the structure exhibited high surface area and nitrogen-rich from in-situ preparation in the structure. From the XPS result, the activated nanoporous carbon pyrolyzed at 800 °C has a pyrrole type form and the activated nanoporous carbon pyrolyzed at 600 °C which has both pyridine and pyrrole type. The carbon which pyrolyzed at 800 °C show higher CO_2 adsorption capacity as shown in table 4.5 because the effect of nitrogen species of pyrrole type has 5 menber ring that has more reactivity than the pyridene type. Thus, the activated nanoporous carbon pyrolyzed at 800 °C was suitable for the carbon-dioxide adsorption process.

Table 4.5 The value of carbon-dioxide adsorption

Sample	CO_2 Adsorption (mmol/g)	N-type
AC-800°C	1.233	Pyrrole
AC-600°C	0.540	Pyrrole and Pyridine

Conclusions

N-rich nanoporous carbon was successfully prepared by pyrolysis process of benzoxazine precursor in an inert atmosphere. Benzoxazine precursor was prepared by sol-gel method using hard template synthesis method to increase the adsorption capacities. The ratio of silica colloidal and CTAB were varied. The nanoporous carbon from polybenzoxazine with 40%wt of silica shows the highest BET surface area of 945 m^2/g and average pore size of 15.44 nm. These results imply that silica can be used to improve the specific surface area and total pore volume by adding in a proper concentration. Moreover, the effect of high surface area and nitrogen-rich nanoporous carbon which pyrrole-type exhibited good adsorption capacity was reported

Acknowledgements

The author is grateful for the scholarship and funding of the thesis work provided by the Petroleum and Petrochemical College; and the Center of Excellence for Petroleum, Petrochemicals, and Advanced Materials, Thailand.

References

[1] Zhi-hong, Tang., Zhuo, Han., Guang-zhi, Yang., Bin, Zhao., Shu-ling, Shen. and Jun-he, Yang. (2013) Preparation of nanoporous carbons with hierarchical pore structure for CO_2 capture. New Carbon Materials, 28, 55-60.

[2] Chen, Chao., Kim, Jun. and Ahn, Wha-Seung. (2012) Efficient carbon dioxide capture over a nitrogen-rich carbon having a hierarchical micro-mesopore structure. Fuel, 95, 360-364.

[3] Tominaka, S., Nakamura, Y. and Osaka, T. (2010) Nanostructured catalyst with hierarchical porosity and large surface area for on-chip fuel cells. Journal of Power Sources, 195(4), 1054–1058.

[4] Rimdusit, S., B.R.C.J. and Dueramae, I. (2012) Characterizations of polybenzoxazine modified with isomeric biphenyltetracarboxylic dianhydrides. eXPRESS Polymer Letters 6, 773-782.

[5] Dueramaea, I., Jubsilpb, C., Takeichic, T. and Rimdusita, S. (2014) High thermal and mechanical properties enhancement obtained in highly filled polybenzoxazine nanocomposites with fumed silica. Composites: Part B, 56, 197-206.

[6] Ghosh, N.N., Kiskan, B. and Yagci, Y. (2007) Polybenzoxazines-New high performance thermosetting resins: Synthesis and properties. Progress in Polymer Science, 32(11), 1344-1391.

[7] Ishida, H. and Allen, D.J. (1996) Physical and mechanical characterization of near-zero shrinkage polybenzoxazines. Journal of Polymer Science Part B: Polymer Physics, 34, 1019-1030.

[8] Katanyoota, P., Chaisuwan, T., Wongchaisuwat, A. and Wongkasemjit, S. (2010) Novel polybenzoxazine-based carbon aerogel electrode for supercapacitors. Materials Science and Engineering B, 167(1), 36-42.

[9] Takeichi, T., Kano, T. and Agag, T. (2005) Synthesis and thermal cure of high molecular weight polybenzoxazine precursors and the properties of the thermosets. Polymer, 46(26), 12172-12180.

[10] Hemvichian, K. and Ishida, H. (2002) Thermal decomposition processes in aromatic amine-based polybenzoxazines investigated by TGA and GC–MS. Polymer, 43, 4391-4402.

[11] Thubsuang, U., Ishida, H., Wongkasemjit, S. and Chaisuwan, T. (2014) Improvement in the pore structure of polybenzoxazine-based carbon xerogels through a silica template method. J Porous Mater, 21, 401-411.

[12] Lin, Q., Dong, S., Qu, L., Fang, C. and Luo, K. (2014) Preparation and properties of ·carbon foam by direct pyrolysis of ally novolak-modified bismaleimide resin. Journal of Analytical and Applied Pyrolysis, 106(0), 164-170.

[13] Lü, Q.-F., He, Z.-W., Zhang, J.-Y. and Lin, Q. (2011) Preparation and properties of nitrogen-containing hollow carbon nanospheres by pyrolysis of polyaniline–lignosulfonate composites. Journal of Analytical and Applied Pyrolysis, 92(1), 152-157.

[14] Lin, Q., Tang, H., Guo, D. and Zheng, M. (2010) Preparation and properties of carbon microbeads by pyrolysis of N-phenyl maleimide modified novolac resin. Journal of Analytical and Applied Pyrolysis, 87(2), 276-281.

[15] Chen, Y., Chen, B.-Z., Shi, X.-C., Xu, H., Hu, Y.-J., Yuan, Y. and Shen, N.-B. (2007) Preparation of pitch-based carbon foam using polyurethane foam template. Carbon, 45(10), 2132-2134.

[16] Wu, D., Fu, R. and Yu, Z. (2005) Organic and carbon aerogels from the NaOH-catalyzed polycondensation of resorcinol–furfural and supercritical drying in ethanol. Journal of Applied Polymer Science, 96(4), 1429-1435.

[17] Liu, Zhen., Dua, Zhenyu., Song, Hao., Wang, Chuangye., Subhan, Fazle., Xing, Wei. and Yan, Zifeng. (2014) The fabrication of porous N-doped carbon from widely available urea formaldehyde resin for carbon dioxide adsorption. Journal of Colloid and Interface Science, 416, 124-132.

[18] Si, Weijiang., Zhoua, Jin., Zhang, Shumei., Lia, Shijiao., Xing, Wei. and Zhuo, Shuping. (2013) Tunable N-doped or dual N, S-doped activated hydrothermal carbonsderived from human hair and glucose for supercapacitor applications. Electrochimica Acta, 107, 391-405.

[19] He, Jiajun., Tob, John., Mei, Jianguo., Bao, Zhenan. and Wilcox, Jennifer. (2014) Facile Synthesis of Nitrogen-Doped Porous Carbon for Selective CO_2 Capture. Energy Procedia, 63, 2144-2151.

[20] Meng, Long-Yue. and Park, Soo-Jin. (2014) Effect of ZnCl2 activation on CO_2 adsorption of N-doped nanoporous carbons from polypyrrole. Journal of Solid State Chemistry 218, 90-94.

[21] Chen, Chao., Kim, Jun. and Ahn, Wha-Seung. (2012) Efficient carbon dioxide capture over a nitrogen-rich carbon having a hierarchical micro-mesopore structure. Fuel 95, 360-364.

[22] Bai, Ruizhu., Yang, Mingli., Hu, Gengshen., Xu, Leqiong., Hu, Xin., Li, Zhiming., Sunli, Wang., Wei, Dai. and Maohong, Fan. (2015) A new nanoporous nitrogen-doped highly-efficient carbonaceous CO_2 sorbent synthesized with inexpensive urea and petroleum coke. Carbon, 81, 465-473.